Palaeontologia Electronica
palaeo-electronica.org

Hadimopanella oezgueli Gedik, 1977: a palaeoscolecidan sclerite useless for taxonomic purposes

Tania Barragán, Jorge Esteve, Diego C. García-Bellido, Samuel Zamora, and J. Javier Álvaro

ABSTRACT

A new assemblage of *Hadimopanella oezgueli* Gedik, 1977 is described from the middle Caesaraugustan (middle Cambrian) part of the Genestosa Member (Oville Formation) in the Cantabrian Mountains, northern Spain. Sclerites occur disarticulated and display distinct diagenetic processes, with authigenic chlorites occluding primary porosity and secondary fissures. Sclerite distribution was controlled by patchy development of epibenthic multispecies clumps on shell (both carbonate and clayey) substrates. A joint biometric and statistical analysis in both dorsal and lateral views of disarticulated sclerites allows characterization of two distinct morphotypes. These are compared with other occurrences of *H. oezgueli* sclerites from other margins of Gondwana and the Siberian Platform, as a result of which, another morphotype is identified. Two main inferences can be drawn: (i) different ventral trunk-sided sclerites of a same scleritome comprise different sclerite morphotypes and (ii) one distinct sclerite morphotype occurs in different genera and species. These results emphasize the idea that the diagnostic features that characterize the parataxon *H. oezgueli* should not be used for (bio) taxonomic classification of palaeoscolecidan scleritomes.

Tania Barragán. Centro de Astrobiología (CSIC/INTA), Ctra. de Torrejón a Ajalvir km 4, 28850 Torrejón de Ardoz, Spain, barragangt@cab.inta-csic.es
Jorge Esteve.Centre of Biology, Earth and Environmental Sciences, University of West Bohemia at Plzeň, 30619 Plzeň, Czech Republic, jorgeves@unizar.es
Diego C. García-Bellido. Environment Institute,School of Earth & Environmental Sciences, University of Adelaide, Adelaide, SA 5005, Australia, Diego.Garcia-Bellido@adelaide.edu.au
Samuel Zamora. Instituto Geológico y Minero de España, c/ Manuel Lasala, 44 - 9º B, 50006 Zaragoza, Spain, s.zamora@igme.es
J. Javier Álvaro. Centro de Astrobiología (CSIC/INTA). Ctra. de Torrejón a Ajalvir km 4, 28850 Torrejón de Ardoz, Spain, alvarobjj@cab.inta-csic.es

Keywords: biometric analysis; parataxonomy; taphonomy; Cambrian; Gondwana

PE Article Number: 17.3.42A

Submission: 26 May 2014. Acceptance: 22 October 2014

Barragán, Tania, Esteve, Jorge, García-Bellido, Diego C., Zamora, Samuel, and Álvaro, J. Javier 2014. *Hadimopanella oezgueli* Gedik, 1977: a palaeoscolecidan sclerite useless for taxonomic purposes. *Palaeontologia Electronica* 17.3.42A: 1-20.
palaeo-electronica.org/content/2014/959-cambrian-sclerites

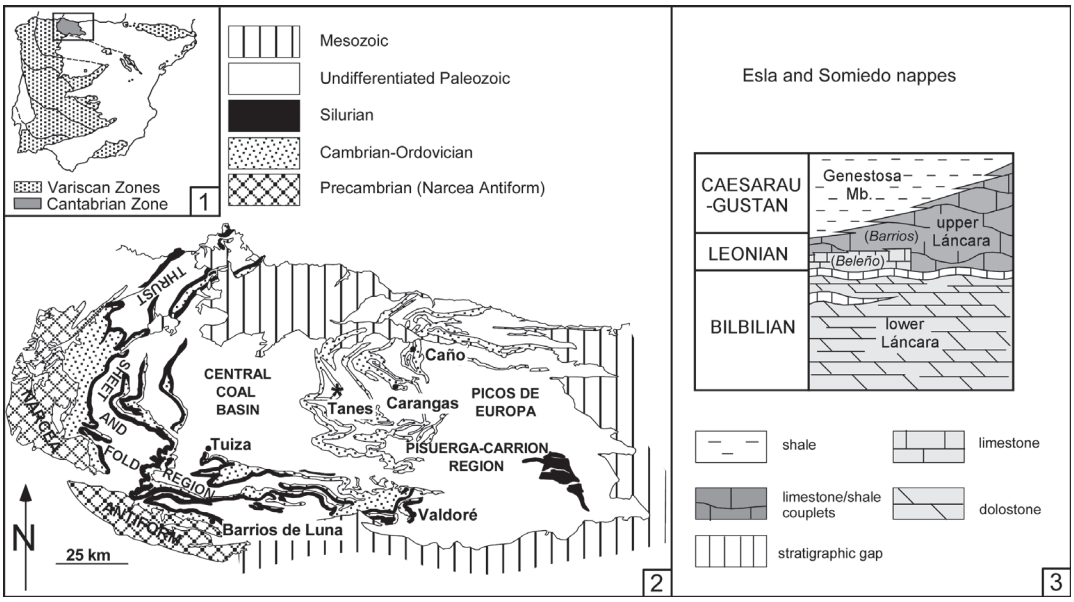

FIGURE 1. (1) Geological sketch of the Iberian Peninsula showing the setting of the Cantabrian Mountains. (2) Geological setting of the study area in Tanes, Cantabrian Mountains. (3) Stratigraphic log of the lower-middle Cambrian transition in the Cantabrian Mountains.

INTRODUCTION

Palaeoscolecids were vermiform metazoans characterized by an annulated long, slender, cylindrical body armoured with organic or organo-phosphatic button-like sclerites arranged in linear patterns. They were common components of Cambrian-Late Silurian marine benthic communities (Conway Morris; 1997; García-Bellido et al., 2013; Hou and Bergström, 1994; Kraft and Mergl, 1989; Müller and Hinz-Schallreuter, 1993; Zhang and Pratt, 1996). Despite the finding of complete and well-preserved palaeoscolecidan cuticles in the lower Cambrian Chengjiang Lagerstätte of China (Hou and Bergström, 1994; Zhang and Pratt, 1996), the middle Cambrian of Australia (Müller and Hinz-Schallreuter, 1993), and the Lower Ordovician of Bohemia (Hinz et al., 1990), some aspects related to both their phylogenetic relationships with ecdysozoan groups and lifestyle are still under discussion (Botting et al., 2012; Conway Morris and Peel, 2010; Han et al., 2007a, 2007b, 2007c; Harvey et al., 2010; Wills et al., 2012).

Their first descriptions were based on compressed body fossils (e.g., Conway Morris and Robison, 1986, Robison, 1969; Ulrich, 1878; Whittard, 1953). Their disarticulated sclerites were found worldwide as dregs after limestone etching with problems to assign them to specific taxa and were described under different generic names, such as *Hadimopanella* Gedik, 1977, *Kaimenella* Märss, 1988 and *Milaculum* Müller, 1973 (e.g., Bendix-Almgreen and Peel, 1988; Bengtson, 1977; Gedik, 1977, 1989; Märss, 1988; Peel and Larsen, 1984; van den Boogard, 1983, 1988, 1989a, 1989b; Wrona, 1982, 1987). They were subsequently integrated with palaeoscolecidan body fossils (Kraft and Mergl, 1989; van den Boogaard, 1989a, 1989b). One well-known cosmopolitan sclerite is *Hadimopanella oezgueli* Gedik, 1977, originally described from Turkey, and significantly abundant in Cambrian sediments of Siberia and Gondwana.

A new assemblage of *Hadimopanella* isolated sclerites from the middle Cambrian of the Cantabrian Mountains (northern Spain) is reported here. The aim of this paper is to offer a quantitative analysis of this assemblage in order to characterize the wide morphological variability of the parataxon. A comparison with other isolated *Hadimopanella* sclerites found elsewhere is provided along with a brief discussion of its (para)taxonomic usefulness. Finally, a discussion of diagenetic processes and palaeoecological constrains is included.

GEOLOGICAL SETTING AND STRATIGRAPHY

The Cantabrian Mountains (Figure 1.1-2) are of prime importance in understanding the benthic community replacements associated with the faunal turnover that characterize the lower-middle Cambrian boundary interval (Álvaro et al., 2013).

The remnants of the subtropical carbonate platform preserved in this part of West Gondwana shows the stepwise record of: (i) the occurrence of the youngest archaeocyathan-microbial reefs of West Gondwana (Perejón and Moreno-Eiris, 2003) associated with ooidal shoal complexes rich in endemic trilobites and low-diversity skeletonized microfossils (Álvaro, 2007; Clausen and Álvaro, 2006); (ii) the onset of a regional erosive unconformity within the Láncara Formation marking the lower-middle Cambrian boundary (Álvaro et al., 2000; Aramburu et al., 1992; Aramburu and García Ramos, 1993; van der Mohr, 1969), bearing an indeterminate biostratigraphic gap laterally correlatable into the Montagne Noire (Wotte et al., 2007); and (iii) the stepwise immigration of new trilobite families, linguliform brachiopods and highly diverse skeletonized microfossils (Clausen and Álvaro, 2006; Sdzuy, 1968, 1995; Wotte, 2006, 2009a, 2009b; Wotte and Mergl, 2007) on middle Cambrian transgressive offshore-dominated substrates.

The occurrence of disarticulated sclerites of *Hadimopanella oezgueli* is related to this earliest mid-Cambrian immigration of shelly fauna. Although its presence was reported from the Barrios (or griotte) facies of the upper Láncara Member (Fernández-Remolar, 2001; van den Boogaard, 1983) (Figure 1.3), unreported limestone interbeds of the overlying Genestosa Member (Oville Formation) are also rife with sclerites. These were sampled in trilobite-rich wackestone-to-packstone tempestites of the Genestosa Member at Tanes (Sdzuy, 1968). The fossiliferous limestones belong to the *Pardailhania hispida* Zone (mid Caesaraugustan) based on its trilobite content (Liñán et al., 1993; Sdzuy, 1968).

MATERIAL AND METHODS

This work is based on a collection of *Hadimopanella oezgueli*-type sclerites sampled after etching of bioclastic limestones from the Genestosa Member and their comparison with other sclerites of the same parataxon previously reported from other margins of Gondwana and the Siberian Platform. Isolated sclerites are used below in their parataxonomic concept, so outside any ortho- or biotaxonomic concept of Bengtson's definition (1985): "a parataxon is a conceptual taxon belonging to a taxonomic system that by formal decision is outside the orthotaxonomic (or biological) system covering the same group of organisms." Only complete palaeoscolecidan scleritomes are reported as (bio)taxonomic entities (Ivantsov and Wrona, 2004), whereas disarticulated sclerites are referred to as parataxons.

In the studied material from the Genestosa Member, 78 sclerites of *H. oezgueli* were selected after etching to carry out biometric and statistical analyses. Smaller specimens, less than 100 µm in diameter, were usually overlooked or hard to extract during picking. Specimens are phosphatic or phosphatized, and usually preserve all the ornamentation details. Several specimens clearly show erosive facets, which are explained later.

Image J-Software (Abràmoff et al., 2004) was used to estimate linear and surface measurements in the dorsal view of sclerites examples from Genestosa Member (n=33) and from other published articles (n=41). Mainly five groups of parameters were measured in dorsal view: (i) largest (D_{max}), shortest (D_{min}), and median (D_{me}=D_{max}+D_{min}/2) diameters of outer surface; (ii) largest (d'_{max}), shortest (d'_{min}), and median (d'_{me}) diameters of middle surface, reported from the outline of the latter (tuberculated surface included); (iii) largest (d_{max}), shortest (d_{min}), and median (d_{me}) diameters of the tuberculated surface, (iv) number of tubercles (no. tubercles) and diameter of largest and smallest tubercles plus their tip diameters (ø largest tubercle, ø smallest tubercle, ø tip); and (v) a measure of eccentricity, based on the distance between the centres of the outer and the tuberculated surface (ed). The relationships built from the latter measures are used in the statistical analyses were: D_{me}/d_{me}, D_{me}-d'_{me}/D, d'-d/D, D_{max}/D_{min}, d_{max}/d_{min}, ed/d_{max}, no. tubercles/d_{me}, ø largest tubercle/ø tip, ø smallest tubercle/ø tip, and ø largest tubercle/ø smallest tubercle. A sketch of main measures is illustrated in Figure 2.1 and a dataset of all these values is specified in Appendices 1, 2 and 3. Several measures were made in lateral view, such as radius of sclerite base (r); heights of marginal brim (h_1), middle surface (h_2), and tuberculated surface (h_3); and slopes of marginal brim (tg α_1), middle surface (tg α_2), and tuberculated surface (tg α_3); as well as the width of tubercle base and tip diameters tubercles and the relationships computed were h/h_1, h/h_2, h/h_3, r/h, tgα_1,tg α_2, tg α_3, and base/tip. The measures are illustrated in Figure 2.2, and their values are included in Appendix 4 and Appendix 5.

Histograms were made to determine the diameter frequency (maximum diameter of the outer surface, D_{max}) measured in dorsal-view specimens and the height frequency (from base to

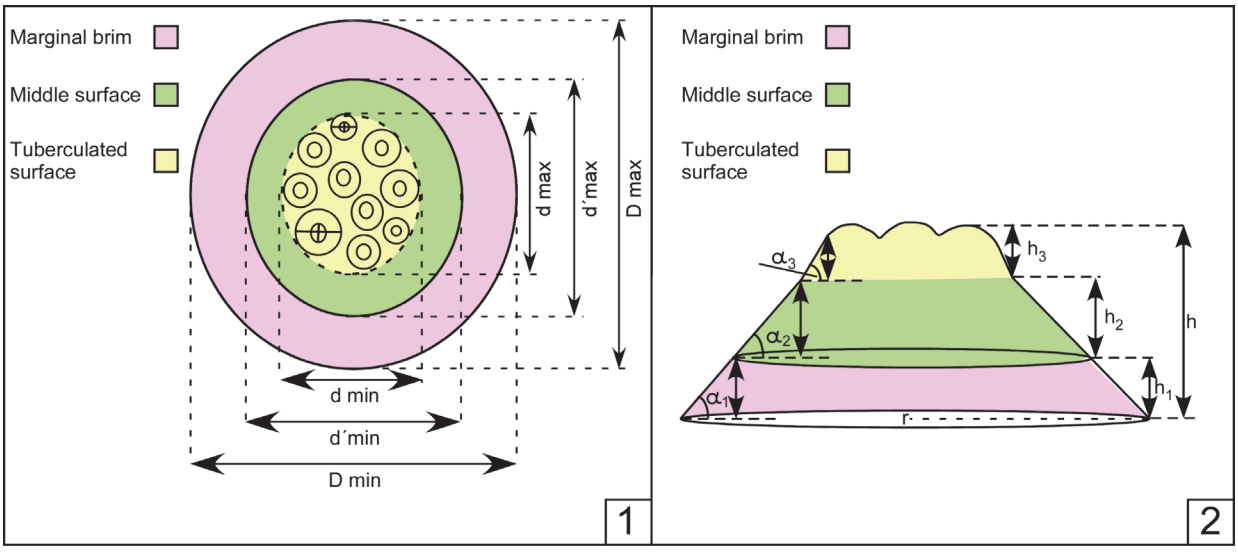

FIGURE 2. Principal parameters measured in dorsal (1) and lateral (2) views of *Hadimopanella oezgueli* sclerites from the Genestosa Member. Abbreviations: largest / shortest diameter of outline sclerite (Dmax/Dmin), middle surface (d´max/d´min) and tuberculated surface (dmax/dmin); height of marginal brim (h_1), middle surface (h_2), and tuberculated surface (h_3); slope of marginal brim (α_1), middle surface (α_2), and tuberculated surface (α_3); radius base (r).

the tip tubercle) measured in lateral-view specimens (Figure 3.1-2); the numerical values of histograms are summarized in Appendix 6.

Cluster analysis (following Ward, 1963) and principal coordinates analysis (PCoA; Gower, 1966) have been carried out to recognize morphotypes in dorsal and lateral views. The cluster analysis illustrated in Figures 4 and 5 include both new sclerites from the Genesosa Member (this work) and other sclerites referred to *H. oezgueli* from the Láncara Formation (van den Boogaard, 1983) in Spain, the Mila Formation of Iran (Wrona and Hamdi, 2001), the Monastery Creek Formation of Australia (Müller and Hinz-Schallreuter, 1993), the Campo Pisano Formation of Sardinia (Elicki, 2006), the Korrelasyonunda Formation (Gedik, 1977), where the holotype was described, and the Çal Tepe Formation (Gedik, 1989; Sarmiento et al., 2001) of Turkey, and the Ülgase-Kallavere Formation of Kirgizia (Märss, 1988). The Siberian sclerites appear in the Sinsk Formation and belong to the following classified species: sclerite from the dorsal side of the trunk (S1) in *Palaeoscolex luboovae* Ivantsov and Wrona, 2004 (*Wronascolex luboovae sensu* Ivantsov and Zhuravlev, 2005; in García-Bellido et al., 2013; Topper et al., 2010), sclerites (S2 and S3) of *Sahascolex labyrinthus* Ivantsov and Wrona, 2004 (*Corrallioscolex labyrinthus sensu* Ivantsov and Zhuravlev, 2005; in Topper et al., 2010), sclerites (S4 and S5) of *Palaeoscolex* sp. Ivantsov and Wrona, 2004 or *Wronascolex* sp. *sensu* Ivantsov and Zhuravlev (2005) (see García-Bellido et al., 2013); Ps1, Ps2, and Ps3 represent different sclerite morphotypes from the ventral side of the trunk of *Palaeoscolex spinosus* Ivantsov and Wrona, 2004 (*Wronascolex spinosus sensu* Ivantsov and Zhuravlev, 2005; in García-Bellido et al., 2013; Topper et al., 2010).

Multivariate analyses were performed by statistics package PAST (Paleontological Statistics) version 1.97 Software (Hammer et al., 2001; Hammer and Harper, 2006).

Finally, spectral imaging by Scanning Electron Microscope (SEM) equipped with an energy-dispersive X-ray spectroscopy (EDS) method was performed to ascertain the chemical composition and to examine the internal structure of some sclerites.

RESULTS

Three statistical analyses of etched sclerites (histogram, cluster, and PCoA analyses) are described below.

Histogram Analysis

Sclerite-size frequency is assessed through dorsal-view measurements (n=33) in Figure 3.1. The observed D_{max} size varies from 120 to 200 µm and the average diameter from 130 to 160 µm,

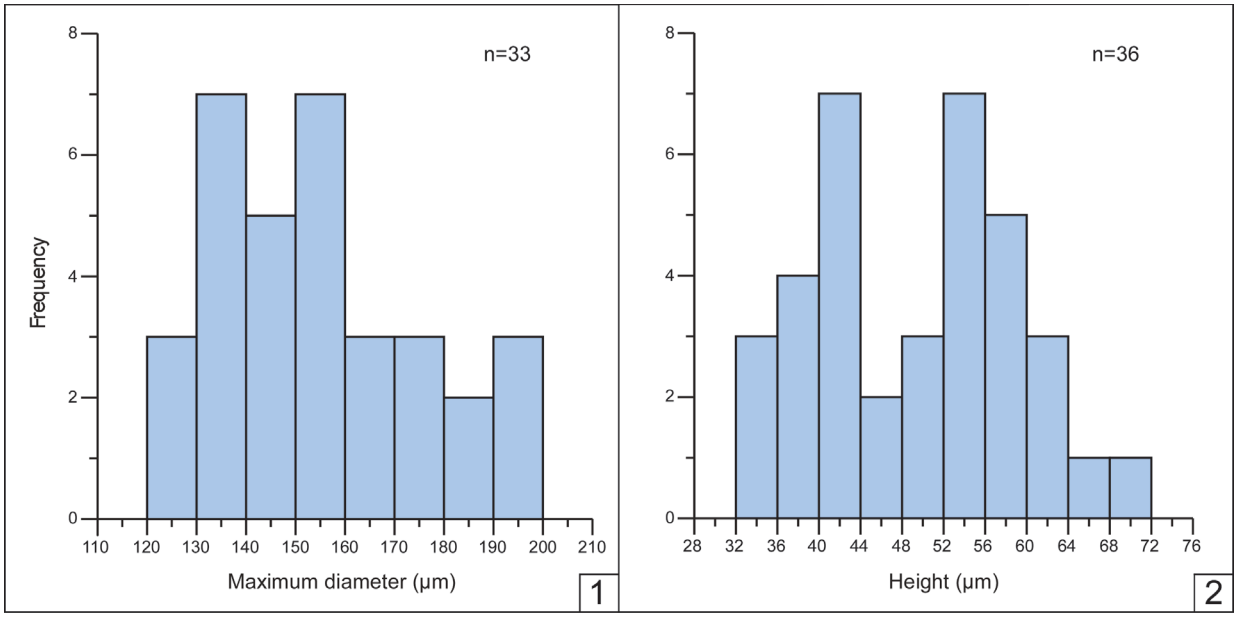

FIGURE 3. (1) Diameter frequency histogram (maximum diameter of outer surface, D max) of dorsal-view sclerites (n=33). (2) Height frequency histogram (from base to the tubercle tip) of lateral-view sclerites (n=36).

which represents 57% of the total selected sclerites. The size range fits well with the average size displayed by similar sclerites from the underlying Upper Láncara Member (van den Boogaard, 1983), with a range of 80–250 µm. The sclerite height frequency histogram measured from the base to the tip of tubercles in lateral view (n=36) is illustrated in Figure 3.2. The height ranges between 32 and 72 µm; although most specimens are broadly distributed in two intervals, between 40–44 µm and 52–60 µm, which represent 52% of the total selected sclerites.

Cluster Analysis

The cluster analysis of dorsal-view sclerites allows identification of two distinct morphotypes (A and B), both subdivided into two submorphotypes, although submorphotypes B is less distinct (Figure 4.1). These are described below following Müller and Hinz-Schallreuter's (1993) nomenclature:

1. Morphotype A (n=16) includes two submorphotypes, A1 (n=3) and A2 (n=13). Submorphotype A1 (Figures 4.1, 5.1-2) includes sclerites with an elliptical and highly eccentric tuberculated surface (or nodular face *sensu* Bengtson, 1977), by comparison with the overall outline. Diameter of A1 sclerites ranges between 149 and 177 µm; they have 7 to 12 tubercles (or nodes) with a basal diameter ranging from 19 to 34 µm in largest tubercles and near 14 µm in smallest tubercles. Most of the tubercles occur on an outer row forming an ellipse with only 1–3 tubercles in the centre; they are very heterogeneous in size and show a markedly sharp tip, and an occasional striated flank; these sclerites present a striated marginal brim, 10–15 µm wide, and a "middle surface", separating the tuberculated surface from the marginal brim, with an irregular width on average 20 µm. Submorphotype A2 (Figures 4.1, 5.3, 5.6-7, 5.10) includes sclerites, 114–191 µm in diameter, with a low eccentric, subelliptical-outlined tuberculated surface, which shows 8–15 tubercles (7–21 µm in diameter for smallest specimens, 16–39 µm in the largest ones); most of the tubercles are mainly placed on an outer row forming a circle or ellipse, although 1–3 tubercles can be closer to the centre. The tubercles are homogeneous in size and have a rounded tip with a striated flank; the brim, 3–31 µm wide, is also striated or grooved and occasionally wavy; the middle surface is subcircular in outline and 10–25 µm wide.
2. Morphotype B (n=17) includes submorphotypes B1 (n=3) and B2 (n=14). Submorphotype B1 sclerites (Figures 4.1, 5.11) are 138–166 µm in diameter and show a rounded and slightly eccentric tuberculated surface. This bears six or seven homogeneous tubercles separated by marked grooves; the marginal brim, 5–20 µm wide, is grooved; the middle

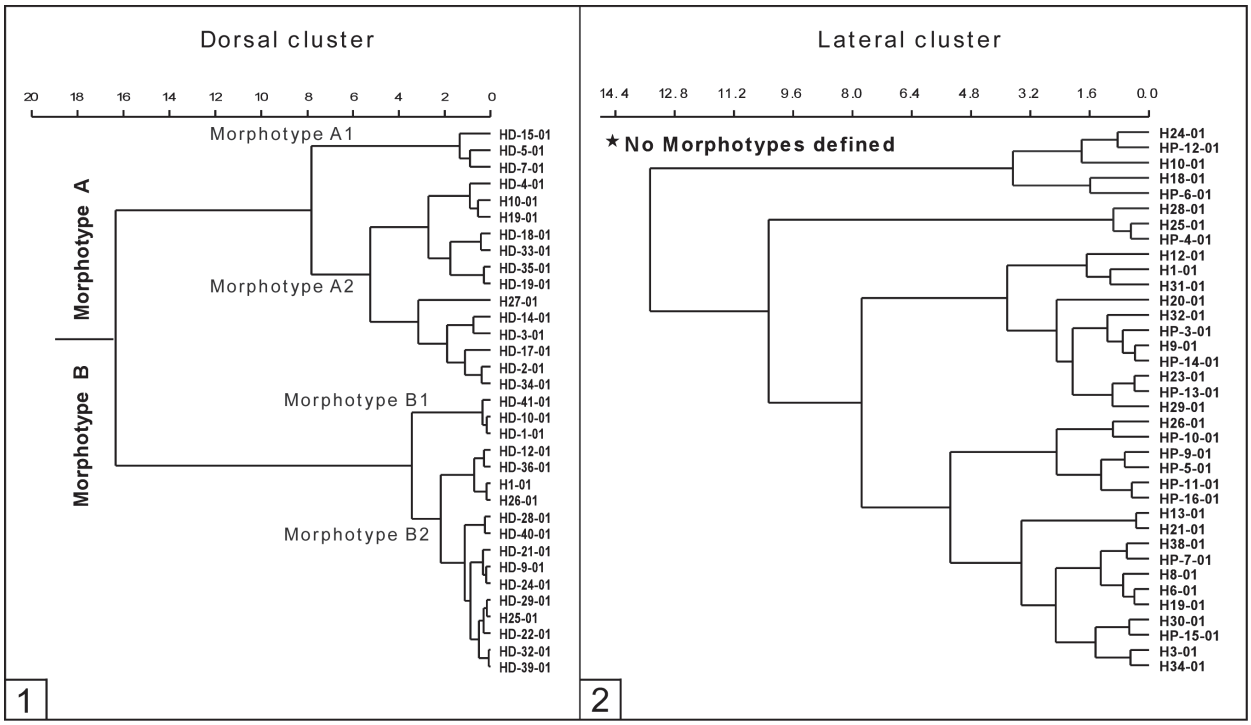

FIGURE 4. (1) Cluster diagram of dorsal-(1) and lateral-view (2) sclerites; morphotypes A1, A2, B1, and B2 are identified in (1), whereas no morphotypes can be recognized in (2).

surface is on average 20 µm wide; this submorphotype has a broad middle surface in comparison with their marginal brim. Sclerites of type B2 (Figure 5.9, 5.14-16) are 116–168 µm in diameter, and show an eccentric and almost round or elliptical tuberculated surface. Some specimens exhibit a flat crest covered by a high number of tubercles (>25), which represents the diagnostic character of *Hadimopanella knappologica* (Bengtson, 1977, Figure 5.9, 5.15). Seven to 28 tubercles form one or two rings surrounding a cluster of up to four tubercles in the centre; the largest diameter of tubercles ranges between 11 and 32 µm and the smallest one between 9 and 23 µm. Tubercles display a high rounded tip and are either heterogeneous in size or homogeneous in the case of sclerites with a high number of tubercles. The brim, 5–17 µm wide, is striated or deeply grooved, and sometimes wavy. The width of the middle surface ranges between 10 and 27 µm on average.

Cluster analysis in lateral-view sclerites (Figure 4.2) does not identify distinct morphotypes. The morphotypes determined in dorsal view show no correlation with lateral morphotypes.

Principal Coordinate Analysis (PCoA)

In order to compare the morphotypes described above with other occurrences of *Hadimopanella oezgueli* from Gondwana and Siberia (see measurements of other illustrated articles sclerites and relationship parameters in Appendices 2-3), a Principal Coordinates Analysis (PCoA) has been carried out with all dorsal-view sclerites (Figure 6.1).

The analysis shows three broad groups (the above-mentioned A1-A2 and B1-B2, and the new C) plus two isolated sclerites (two ventral trunk-sided sclerites of *W. spinosus*, Ps1 and Ps2). The sclerites yielded by the Genestosa limestone interbeds fall into groups A and B; those from the Láncara and Ülgase-Kallavere formations into groups A, B, and C; those from the Mila and Monastery Creek formations into groups A and C; that from the Campo Pisano Formation into group A; and those from Turkey into group C.

The Siberian sclerites are distributed as follows: S and Ps3 (or "*Hadimopanella oezgueli*"-type) in groups A and C and sclerites Ps1 ("spiny coronata"-type) and Ps2 ("*knappologica*"-type; Bengtson, 1977) plot outside the three groups. As a result, different ventral-side trunk sclerites of a same scleritome comprise different sclerite mor-

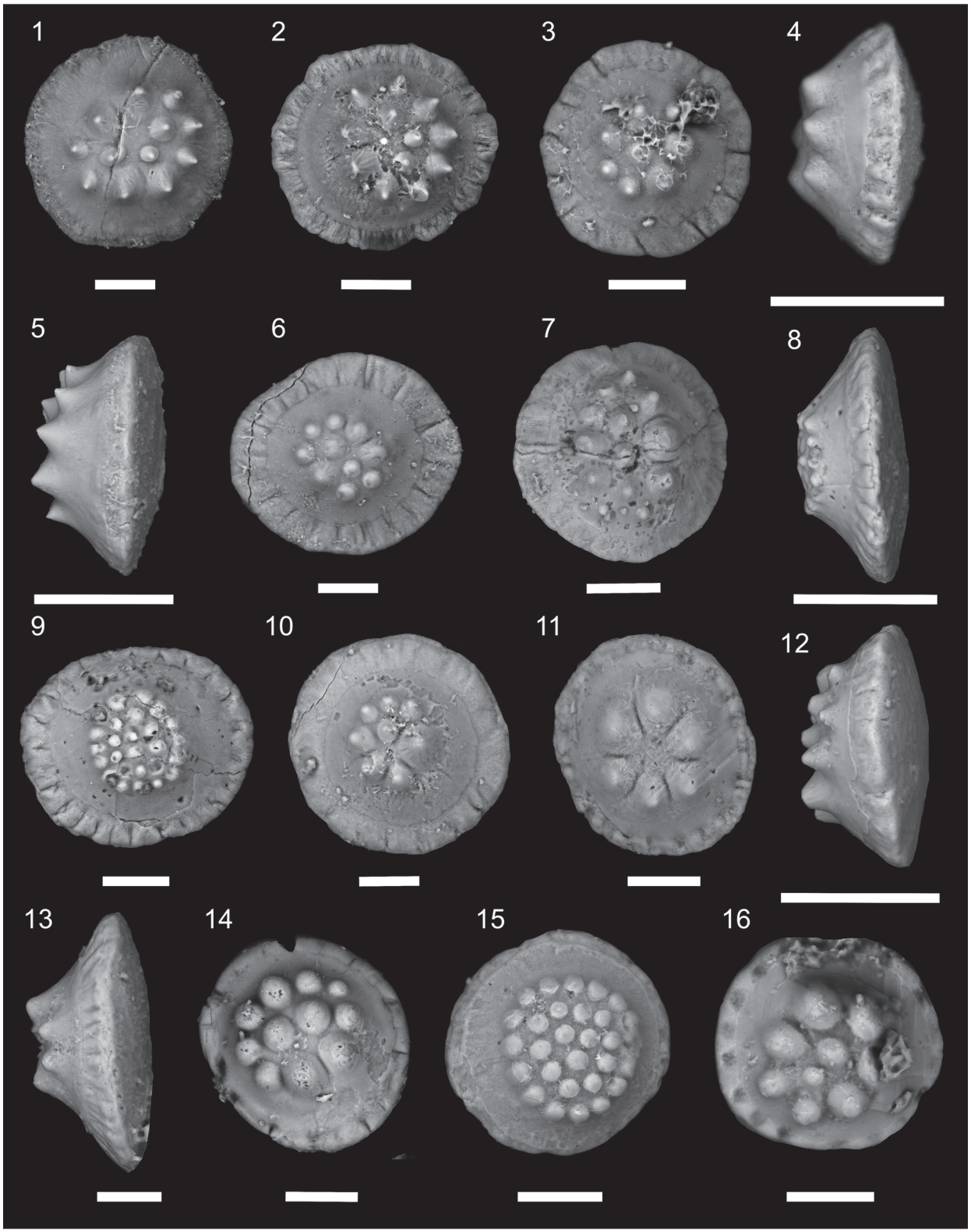

FIGURE 5. (1 to 16) SEM photographs of *Hadimopanella oezgueli* Gedik, 1977 sclerites from the Genestosa Member, middle Caesaraugustan. (1–2) Morphotype A1; (3, 6–7, 10) Morphotype A2; (11) Morphotype B1; (9, 14–16) Morpthotype. B2. (4–5, 8, 12–13) Lateral-view of sclerites; scale bars for dorsal views equal 50 µm and for lateral views scale bars equal 100 µm (except no. 13 =50µm). Illustrated specimens are housed in the Instituto Geológico y Minero de España (IGME: MGM prefix), Spain: from MGM 1118K to MGM 1133K.

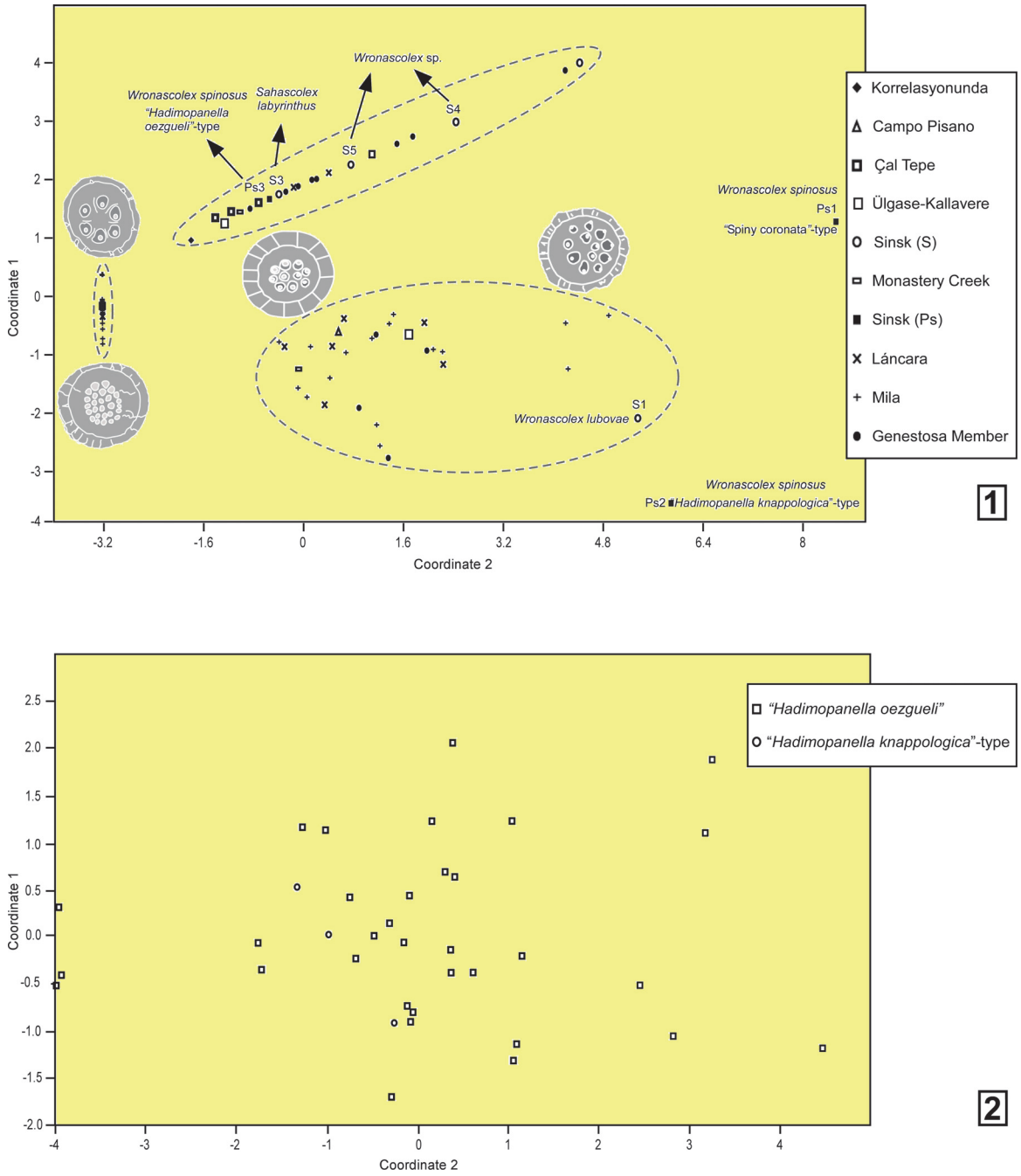

FIGURE 6. (1) Principal-coordinates diagram of dorsal-view sclerites from the Genestosa Member compared with other occurrences of *Hadimopanella oezgueli* Gedik, 1977 from Gondwana and Siberia. (2) Principal-coordinates diagram of lateral-view sclerites from the Genestosa Member with indication of "*Hadimopanella knappologica*"-type sclerites.

photypes, whereas one distinct sclerite morphotype occurs in different genera and species, as has been demonstrated in the case of *W. spinosus*, *W.* sp., and *S. labyrinthus*.

A statistic test of consistency was applied to the above analysis based on ANOSIM (Analysis of Similarities) test. ANOSIM is a non-parametric test to differentiate groups of multivariate data points (Hammer and Harper, 2006). It was applied to the two superclusters (morphotypes) identified above: with 1000 permutations, and using chord, Bray-Curtis, Morista, and Euclidean distance measures, the test statistic is consistently high (R=0.91–0.96) and the p value remains <0.0001, proving signifi-

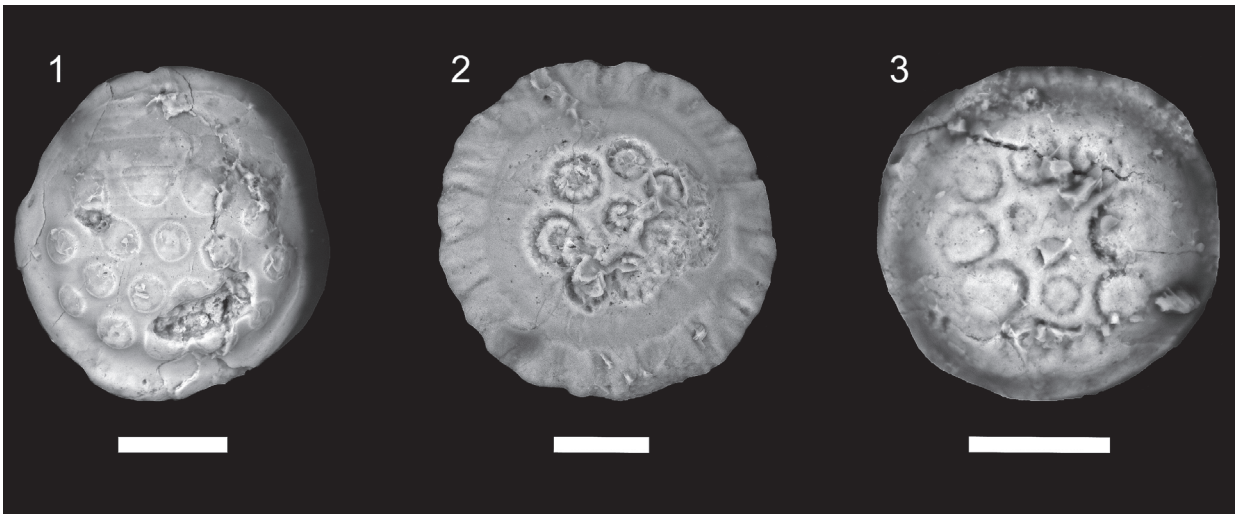

FIGURE 7. (1–3) Dorsal views of sclerites with eroded tubercles; only specimen 2 preserves its original marginal brim. Scale bars equal 50 µm (MGM 1134K to MGM 1136K).

cant differences between groupings and thus supporting the result of the cluster analysis.

By contrast, the principal coordinates diagram performed with lateral-view sclerites does not show any distinctive morphotypes (Figure 6.2). In general, all the samples are dispersed in a cloud. Some "*Hadimopanella knappologica*"-type sclerites may be distinctly identified in this diagram owing to their characteristic flat crest and high number of tubercles (Figure 5.8).

TAPHONOMIC CONSTRAINTS

Some sclerites display eroded facets, mainly affecting tubercles, whereas others exhibit both tubercles and marginal brim eroded (Figure 7.1-3). Selective abrasion of tubercles could be explained by ultrastructure and growth patterns, as tubercles are easily susceptible to loss in life of palaeoscolecids since they grow by molting. The old cuticles overlying the new ones show tubercles dramatically eroded by friction (Müller and Hinz-Schallreuter, 1993: text figure 14) (Figure 7.2). In addition, eroded tubercles may reflect transport prior to definitive burial, which is consistent with their occurrence in storm-induced deposits.

The presence of chlorites both on the surface and within the *Hadimopanella* sclerites is well constrained by SEM analysis. The surface is rife with authigenic chlorites displayed in a honey-comb arrangement (Figure 8.1). In broken and corroded specimens, chlorite crystals occur seemingly replacing the original apatite (Figure 8.2). In addition, these chlorites also occur occluding internal fissure networks, clearly recognized in SEM by their darker grey color (Figure 8.5). The cross-section of a well-preserved sclerite (Figure 8.3) allows identification of chlorite distribution in a selective way, depending on porosity or cracking in each surface area so that, in BSE analyses, chlorites (recognisable by mapping of Fe and Mg in yellow and white, respectively, Figure 8.4), are preferably located covering the tuberculated surface and the base of the marginal brim. In contrast, pristine apatite (see mapping of P and Ca elements in turquoise and white, respectively), which could represent the primary biomineral cuticle of the palaeoscolecids (Harvey et al., 2010), forms the surface of the middle surface and the marginal brim. As a result, the preservation after diagenetic mineral replacement can be explained by its non-porous and massive character: the resulted phosphatic parts of the sclerite were less susceptible to be damaged by abrasion and affected by cement occlusion. In Figure 8.6, BSE of a crosscut specimen (see picture by SEM in Figure 8.5), has distinct chlorites occluding internal fissures, represented by Fe-Al in yellow and white, and original apatite composition, illustrated by P–Ca colors (turquoise and white, respectively).

CALM CLAYEY VS ENERGETIC SHELLY SUBSTRATES

Two types of middle Cambrian limestones have yielded *Hadimopanella* sclerites in the Cantabrian Mountains: the Barrios facies of the upper Láncara Member (van den Boogaard, 1983) and the interbedded storm-induced limestones of the

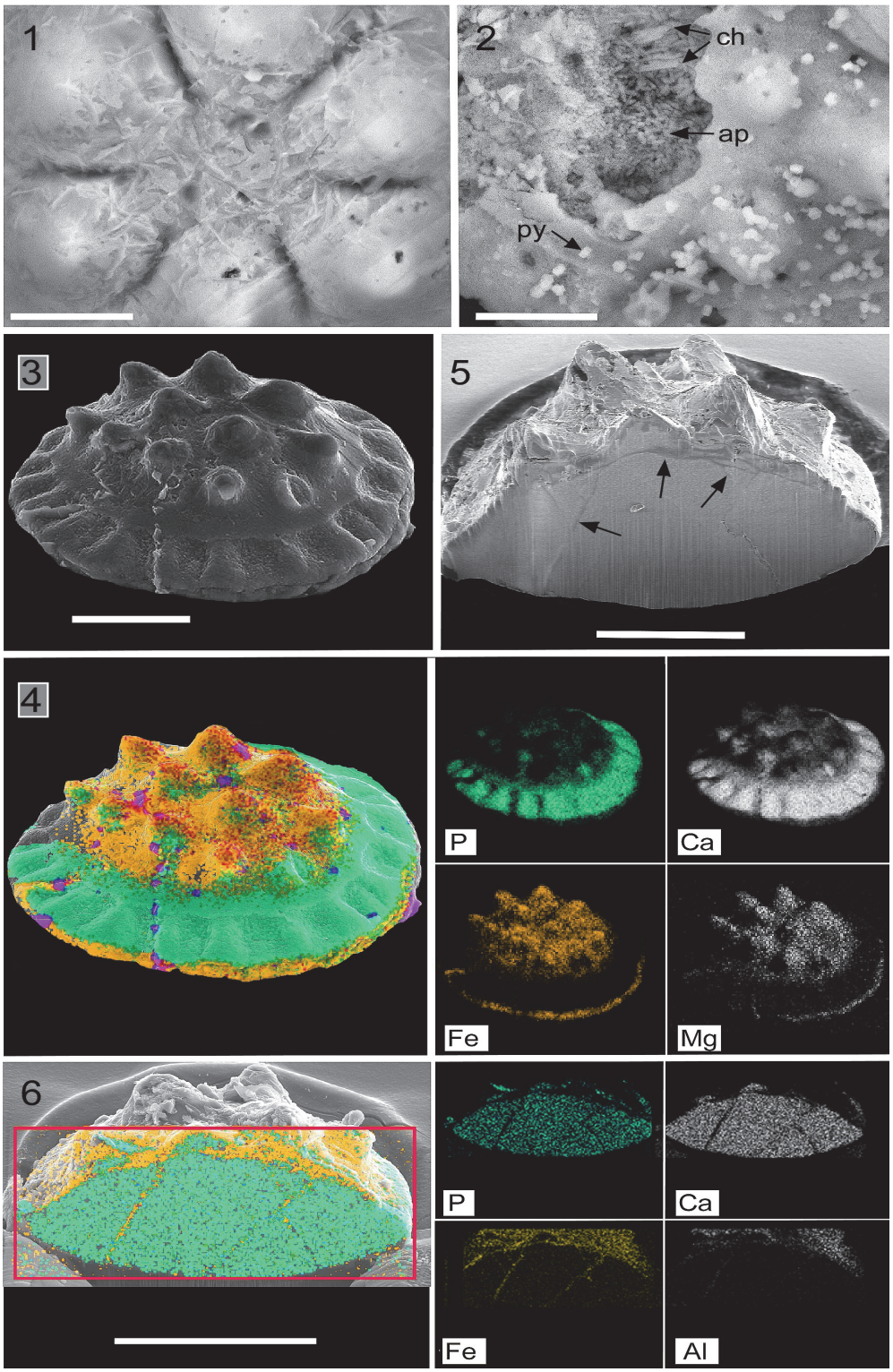

FIGURE 8. Fig. (1) Honey-comb arrangement of chlorites on the top of a sclerite (detail of Figure 5.11) MGM 1128K. (2) Chlorites embedded in the apatite (ap) framework of a corroded sclerite (arrowed) with diagenetic crystals of pyrite (py) and chlorite (ch), MGM 1104K. (3) Complete sclerite, MGM 1137K. (4) BSE analysis of previous sclerite with chlorite arrangement marking porous and fissured areas. (5). Lateral section of sclerite showing fissure network (arrowed), MGM 1138K. (6) BSE analysis of previous sclerite with chlorites occluding the internal fissure network. Scale bars: 1-2 equal 20 µm; 3-4 equal 100 µm; 5 equals 40 µm; 6 equals 60 µm.

overlying Genestosa Member, Oville Formation (this paper).

The Barrios or griotte facies, up to 30 m thick, consists of centimetre-thick alternations of reddish to purple, nodular and bedded limestone/shale couplets. They represent episodes of shelly carbonate productivity on synsedimentary palaeohighs, finally sealed by the shale-dominated Genestosa Member. Drowning and subsequent transgression of the palaeohighs led to a distinct change in benthic fauna, from echinoderm-rich to trilobite-brachiopod-rich fossil assemblages (Wotte, 2009b). *Hadimopanella* sclerites were found in the upper part of the Barrios facies in Los Barrios de Luna and Valdoré (Fernández-Remolar, 2001, van den Boogaard 1983) in shelly substrates representative of shoreface environments under persistent wave action (Álvaro et al., 2000; Álvaro and Clausen, 2005; Wotte et al., 2007).

The Genestosa Member, c. 350 m thick, consists of burrowed greenish claystone beds with abundant centimetre- to decimetre-thick carbonate interbeds and nodules, including shelly wackestone-packstone and laminated calcisiltites. Carbonate interbeds provide evidence for episodic storm deposits. The general depositional environment of the Genestosa Member is envisaged as an offshore-dominated, gently northwardly sloping clayey shelf. The platform bordered in the SE with a sandy shoreline that diachronously prograded leading to the onset of sandstone wedge interbeds (e.g., the so-called “simula sandstone”; Zamarreño, 1972). The episodic record of vigorous burrowing, among other factors, allowed sedentary fauna (mainly eocrinoids and sponges) to proliferate. Turbidity was another limiting factor due to the coexistence of autochthonous epibenthic assemblages of normal-eyed and blind trilobites (the so-called conocoryphid biofacies; Álvaro and Vizcaïno, 2003). In bottom conditions of increasing sedimentation rates and turbidity, muds lacking cohesion are easily re-suspended to generate high-turbidity conditions. As a result, mud suspended in water may have greatly reduced the amount of light reaching the seafloor, and dark to dimly lit substrate conditions may be formed.

Errant palaeoscolecids were vagile colonizers of both high-energy shelly substrates (firm carbonate substrates consolidated by early-diagenetic cementation processes, see Zamora et al., 2010) and low-energy clayey substrates (subsequently reworked by tempestites) across the Leonian-Caesaraugustan. Their preservation is not dependent on the kind of seafloor, but on taphonomic constraints. Both wave and storm action exerted their influence upon benthic communities and must be considered as primary agents of substrate modification and episodic physical disturbances. Storms generated winnowing leading to shell-bed formation by initiating shelly pavements on an otherwise soft substrate. This distribution resulted in the patchy development of epibenthic multispecies clumps on shell grounds.

DISCUSSION AND CONCLUSIONS

Sclerites of *Hadimopanella oezgueli* yielded by the Genestosa limestone interbeds (middle Cambrian) of the Oville Formation (Cantabrian Mountains) show a widespread morphological variability. Variable parameters include the number of dorsal tubercles (a single circle with 2–15 tubercles) and a variable number of central tubercles (even their absence); a variable eccentricity of the tuberculate surface; a variable relative width of the marginal brim, middle, and tuberculated surfaces; and a variable diameter and upper end (acute *vs* rounded) of dorsal tubercles.

The taxonomic connection between disarticulated sclerites and scleritomes depends on the proper preservation of the former and statistical analyses, like those made in this paper. These allow characterization of parataxonomic diversity in a same stratigraphic level. After statistical comparison with other palaeoscolecidan taxa bearing sclerites of *H. oezgueli*, it is possible to conclude that different ventral-sided sclerites of a same scleritome comprise different (ventral trunk) sclerite morphotypes, whereas one distinct sclerite morphotype occurs in different genera and species. These results confirm in a representative way that the diagnostic features that characterize the parataxon *H. oezgueli* have serious difficulties to establish any (bio)taxonomic classification for palaeoscolecidan (scleritome-based) worms. Therefore, the diagnostic characters of isolated sclerites, such as those of the parataxon *H. oezgueli*, must be not taken into consideration for diagnosing scleritome taxa, and the parataxon *H. oezgueli* should not be used for (bio) taxonomic purposes.

Two parallel taxonomic classifications are currently applied to palaeoscolecidan complete scleritomes and disarticulated sclerites. Three sclerite-based parataxa are formally erected, *Milaculum*, *Hadimopanella* and *Kaimenella* (e.g., Gedik, 1977; Hinz et al., 1990; Müller, 1973; van de Boogaard, 1983), based on specific external ornamentation patterns. By contrast, taxonomy of complete scler-

itomes (Bengtson, 1985) has been achieved based on partial scleritome. Although the ontogeny of palaeoscolecids is suspected to be complex (Botting et al., 2012; Brock and Cooper, 1993; Topper et al., 2010), the transition from juvenile to adult stages is not characterized by any significant change in the shape or size of sclerites. Only the interspace between single plates gradually increases during the ontogeny because of an incomplete development of cuticular structures (Zhuravlev et al., 2011).

The occurrence of palaeoscolecidan sclerites does not depend on the kind of substrate (clayey *vs*. shelly) since palaeoscolecids lived on both calm and energetic substrates. By contrast, their abundance is dramatically constrained by taphonomic processes (including occlusion of diagenetic fissures by chlorite) and the possibility of etching extraction.

ACKNOWLEDGEMENTS

The authors thank the useful revision made by two anonymous referees. This paper is a contribution to projects CGL2010-19491, CGL2013-48877 and GCL2011-24516 from Spanish MINECO and EU-FEDER. J.E. is supported by European Social fund and Ministry of Education Youth and Sport, Czech Republic (Ref.CZ. 1.07/2.3.00/30.0013). S.Z. is funded by a Ramón y Cajal Grant (RYC-2012-10576).

REFERENCES

Abràmoff, M.D., Magalhães, P.J., and Ram, S.J. 2004. Image processing with ImageJ. *Biophotonics International*, 11(7):36–42.

Álvaro, J.J. 2007. New ellipsocephalid trilobites from the lower Cambrian member of the Láncara Formation, Cantabrian Mountains, northern Spain. *Memoirs of the Association of Australasian Palaeontologists*, 34:343–355.

Álvaro, J.J. and Clausen, S. 2005. Major geodynamic and sedimentary constraints on the chronostratigraphic correlation of the Lower-Middle Cambrian transition in the western Mediterranean region. *Geosciences Journal,* 9:145–160.

Álvaro, J.J. and Vizcaïno, D. 2003. The conocoryphid biofacies, a benthic assemblage of normal-eyed and blind trilobites. *Special Papers on Palaeontology*, 70:127–140.

Álvaro, J.J., Vennin, E., Moreno-Eiris, E., Perejón, A., and Bechstädt, T. 2000. Sedimentary patterns across the Lower-Middle Cambrian transition in the Esla nappe (Cantabrian Mountains, northern Spain). *Sedimentary Geology*, 137:43–61.

Álvaro, J.J., Zamora, S., Clausen, S., Vizcaïno, D. and Smith, A.B. 2013. The role of abiotic factors in the Cambrian Substrate Revolution: A review from the benthic community replacements of West Gondwana. *Earth-Science Reviews*, 118:69–82.

Aramburu, C. and García Ramos, J.C. 1993. La sedimentación cambro-ordovícica en la Zona Cantábrica (NO de España). *Trabajos de Geología, Universidad de Oviedo*, 19:45–73.

Aramburu, C., Truyols, J., Arbizu, M., Méndez-Bedia, I., Zamarreño, I., García-Ramos, J. C., Suárez de Centi, C., and Valenzuela, M. 1992. El Paleozoico Inferior de la Zona Cantábrica. p. 397–422. In Gutiérrez-Marco, J.C., Saavedra, C. and Rábano, I. (eds.), *Paleozoico Inferior de Ibero-América*, UNEX Press, Mérida.

Bendix-Almgren, S.E. and Peel, J.S. 1988. *Hadimopanella* from the Lower Cambrian of North Greenland: structure and affinities. *Bulletin of the Geological Society of Denmark*, 37:83–103.

Bengtson, S. 1977. Early Cambrian button-shaped phosphatic microfossils from the Siberian Platform. *Palaeontology*, 20:751–762.

Bengtson, S. 1985. Taxonomy of disarticulated fossils. *Journal of Paleontology*, 59:1350–1358.

Botting, J.P., Muir, L.A., Van Roy, P., Bates, D., and Upton, C. 2012. Diverse Middle Ordovician palaeoscolecidan worms from the Builth-Llandrindod inlier of central Wales. *Palaeontology*, 55:501–528.

Brock, G.A. and Cooper, B.J. 1993. Shelly fossils from the Early Cambrian (Toyonian) Wirrealpa, Aroona Creek, and Ramsay limestones of South Australia. *Journal of Paleontology*, 67:758–787.

Clausen, S. and Álvaro, J.J. 2006. Skeletonized microfossils from the Lower-Middle Cambrian transition of the Cantabrian Mountains, northern Spain. *Acta Palaeontologica Polonica*, 51:223–238.

Conway Morris, S. 1997. The cuticular structure of the 495-Myr-old type species of the fossil worm *Palaeascolex*, *P. piscatorum* (?Priapulida). *Zoological Journal of the Linnean Society*, 119:69–82.

Conway Morris, S. and Peel, J.S. 2010. New palaeoscolecidan worms from the Lower Cambrian: Sirius Passet, Latham Shale and Kinzers Shale. *Acta Palaeontologica Polonica*, 55:141–156.

Conway Morris, S. and Robison, R.A. 1986. Middle Cambrian priapulids and other soft-bodied fossils from Utah and Spain. *University of Kansas Paleontological Contributions*, 9:1–22.

Elicki, O. 2006. Microbiofacies analysis of Cambrian offshore carbonates from Sardinia (Italy): environment reconstruction and development of a drowning carbonate platform. *Carnets de Géologie*, 2006:1–26.

Fernández-Remolar, D. 2001. Nota sobre la distribución estratigráfica de *Hadimopanella* Gedik, 1977 (microescleritos de paleoscolécidos), en el Cámbrico. *Revista Española de Micropaleontología*, 33:113–121.

García-Bellido, D.C., Paterson, J.R., and Edgecombe, G.D. 2013. Cambrian palaeoscolecids (Cycloneuralia) from Gondwana and reappraisal of species assigned to *Palaeoscolex. Gondwana Research,* 24:780–795.

Gedik, I. 1977. Conodont stratigraphy in the Middle Taurus. *Bulletin of the Geological Society of Turkey*, 20:35–48. (In Turkish)

Gedik, I. 1989. Hadimopanellid biostratigraphy in the Cambrian of the Western Taurids: A new biostratigraphic tool in the subdivision of Cambrian System. *Geological Bulletin of Turkey*, 32:65–78. (In Turkish)

Gower, J.C. 1966. Some distance properties of latent root and vector methods used in multivariate analysis. *Biometrika*, 53:325–338.

Hammer, Ø. and Harper, D.A.T. 2006. *Paleontological Data Analysis*. Blackwell, Oxford, 351 p.

Hammer, M.F., Karafet M.T., Redd A.J., Jarjanazi H., Santachiara-Benerecetti, A.S., Soodyall, H., and Zegura, S.L. 2001. Hierarchical patterns of global human Y-chromosome diversity. *Molecular Biology Evolution*, 18:1189–1203.

Han, J., Liu, J.N., Zhang, Z.F., Zhang, X.L., and Shu, D.G. 2007a. Trunk ornamentation on the palaeoscolecid worms *Cricocosmia* and *Tabelliscolex* from the Early Cambrian Chengjiang deposits of China. *Acta Palaeontologica Polonica*, 52:423–431.

Han, J., Yang, Y., Zhang, Z.F., Liu, J.N., and Degan, D.G. 2007b. New observations on the palaeoscolecid worm *Tylotites petiolaris* from the Cambrian Chengjiang Lagerstatte, south China. *Paleontological Research*, 11:59–69.

Han, J., Zhang, Z.F., Liu, J., and Shu, D.G. 2007c. Evidence of priapulid scavenging from the Early Cambrian Chengjiang deposits, Southern China. *Palaios*, 22:691–694.

Harvey, T.H.P., Dong, X.P., and Donoghue, P.C.J. 2010. Are palaeoscolecids ancestral ecdysozoans? *Evolution & Development*, 12:177–200.

Hinz, I., Kraft, P., Mergl, M., and Müller, K.J. 1990. The problematic *Hadimopanella*, *Kaimenella*, *Milaculum* and *Utahphospha* identified as sclerites of Palaeoscolecida. *Lethaia*, 23:217–221.

Hou, X. and Bergström, J. 1994. Palaeoscolecid worms may be nematomorphs rather than annelids. *Lethaia*, 27:11–17.

Ivantsov, A.Yu. and Wrona, R. 2004. Articulated palaeoscolecid sclerite arrays from the Lower Cambrian of eastern Siberia. *Acta Geologica Polonica*, 54:1–22.

Ivantsov, A.Yu. and Zhuravlev, A.Yu. 2005. Cephalorhynchs, p. 61–72. In Pomarenko, A.G. (ed.), *Unikalnye sinskiye mestonakhozhdeniya rannekembriyskikh organizmov*. Trudy Paleontologicheskogo Instituta, Moscow. (In Russian)

Kraft, P. and Mergl, M. 1989. Worm-like fossils (Palaeoscolecida; ?Chaetognatha) from the Lower Ordovician of Bohemia. *Sborník geologických věd Paleontologie*, 30:9–36.

Liñán, E., Perejón, A., and Sdzuy, K. 1993. The Lower-Middle Cambrian stages and stratotypes from the Iberian Peninsula: a revision. *Geological Magazine*, 130:817–833.

Märss, T. 1988. Early Palaeozoic hadimopanellids of Estonia and Kirgizia (USSR). *Proceedings of the Academy of Sciences of the Estonian SSP, Geology*, 37:10–17.

Müller, K.J. 1973. *Milaculum* n. gen., ein phosphatisches Mikrofossil aus dem Altpalaeozoikum. *Paläontogische Zeitschrift*, 47:217–228.

Müller, K.J. and Hinz-Schallreuter, I. 1993. Palaeoscolecid worms from the Middle Cambrian of Australia. *Palaeontology*, 36:543–592.

Peel, J.S. and Larsen, N.H. 1984. *Hadimopanella apicata* from the Lower Cambrian of western North Greenland. *Rapport Grønlands Geologiske Undersøgelse*, 121:89–96.

Perejón, A. and Moreno-Eiris, E. 2003. Arqueociatos del Bilbiliense (Cámbrico Inferior) del manto del Esla, Cordillera Cantábrica, Norte de España. *Boletín de la Real Sociedad Española de Historia Natural (Sección Geológica)*, 98:51–71.

Robison, R.A. 1969. Annelids from the Middle Cambrian Spence Shale of Utah. *Journal of Paleontology*, 43:1169–1173.

Sarmiento, G.N., Fernández-Remolar, D., and Göncüoglu, C. 2001. Cambrian small shelly fossils from the Çal Tepe Formation, Taurus Mountains, Turkey. *Coloquios de Paleontología*, 52:117–134.

Sdzuy, K. 1968. Trilobites del Cámbrico Medio de Asturias. *Trabajos de Geología, Universidad de Oviedo*, 1:77–135.

Sdzuy, K. 1995. Acerca del conocimiento actual del Sistema Cámbrico y del límite Cámbrico Inferior-Medio, p. 253–263. In Gámez Vintaned, J.A. and Liñán, E. (eds.), *La expansión de la vida en el Cámbrico*. Institución 'Fernando el Católico', Zaragoza.

Topper, T.P., Brock, G.A., Skovsted, C.B., and Paterson, J.R. 2010. Palaeoscolecid scleritome fragments with *Hadimopanella* plates from the early Cambrian of South Australia. *Geological Magazine*, 147:86–97.

Ulrich, E.O. 1878. Observations on fossil annelids and descriptions of some new forms. *Journal of the Cincinnati Society of Natural History*, 1:87–91.

van den Boogaard, M. 1983. The occurrence of *Hadimopanella oezgueli* Gedik in the Láncara Formation in NW Spain. *Proceedings of the Koninklijde Nederlandse Akademie van Wetenschappen Series B*, 86:331–341.

van den Boogaard, M. 1988. Some data on *Milaculum* Müller, 1973. *Scripta Geologica*, 88:1–25.

van den Boogaard, M. 1989a. A problematic microfossil, *Hadimopanella*? *coronata* sp. nov., from the Ordovician of Estonia. *Rijksmuseum van Geologie en Mineralogie Series B*, 92:179–190.

van den Boogaard, M. 1989b. Isolated tubercles of some Palaeoscolecida. *Scripta Geologica,* 90:1–12.

van der Meer Mohr, C.G. 1969. The stratigraphy of the Cambrian Láncara Formation between the Luna river and the Esla river in the Cantabrian Mountains, Spain. *Leidse Geologische Mededelingen*, 43:233–316.

Ward, J.H. 1963. Hierarchical grouping to optimize an objective function. *Journal of the American Statistical Association*, 58:236–244.

Whittard, W.F. 1953. *Palaeoscolex piscatorum* gen. et sp. nov., a worm from the Tremadocian of Shropshire. *Quarterly Journal of the Geological Society of London*, 109:125–35.

Wills, M.A., Gerber, S., Ruta, M., and Hughes, M. 2012. The disparity of priapulid, archaeopriapulid and palaeoscolecid worms in the light of new data. *Journal of Evolutionary Biology*, 25:2056–2076.

Wotte, T. 2006. New Middle Cambrian molluscs from the Láncara Formation of the Cantabrian Mountains (north-western Spain). *Revista Española de Paleontología*, 21:145–158.

Wotte, T. 2009a. The youngest cambroclaves: *Cambroclavus absonus* from the Middle Cambrian of the Cantabrian zone (northwest Spain). *Journal of Paleontology*, 83:128–134.

Wotte, T. 2009b. Re-interpretation of a Lower-Middle Cambrian West Gondwanan ramp depositional system: a case study from the Cantabrian Zone (NW Spain). *Facies,* 55:473–487.

Wotte, T. and Mergl, M. 2007. Brachiopods from the Lower-Middle Cambrian Láncara Formation of the Cantabrian Mountains, Northwest Spain. *Memoirs of the Association of Australasian Palaeontologists*, 33:101–122.

Wotte, T., Álvaro, J.J., Shields, G.A., Brasier, M., and Veizer, J. 2007. C-, O- and Sr-isotope stratigraphy across the Lower-Middle Cambrian transition of the Cantabrian Mountains (Spain) and the Montagne Noire (France), West Gondwana. *Palaeogeography, Palaeoclimatology, Palaeoecology*, 256:47–70.

Wrona, R. 1982. Early Cambrian phosphatic microfossils from southern Spitsbergen (Horsund region). *Palaeontologia Polonica*, 43:9–16.

Wrona, R. 1987. Cambrian microfossil *Hadimopanella* Gedik from glacial erratics in West Antarctica. In Gazdzicki, A. (ed.), Palaeontological Results of the Polish Antarctic Expeditions, Part I. *Palaeontologia Polonica*, 49:37–48.

Wrona, R. and Hamdi, B. 2001. Palaeoscolecid sclerites from the Upper Cambrian Mila Formation of the Shahmirzad section, Alborz Mountains, northern Iran. *Acta Geologica Polonica*, 51:101–107.

Zamarreño, I. 1972. Las litofacies carbonatadas del Cámbrico de la Zona Cantábrica (NW España) y su distribución paleogeográfica. *Trabajos Geológicos, Universidad de Oviedo*, 5:1–118.

Zamora, S., Clausen, S., Álvaro, J.J., and Smith, A.B. 2010. Pelmatozoan echinoderms as colonizers of carbonate firmgrounds in mid-Cambrian high energy environments. *Palaios*, 25:764–768.

Zhang, X.G. and Pratt, B.R. 1996. Early Cambrian palaeoscolecid cuticles from Shaanxi, China. *Journal of Paleontology*, 70:275–279.

Zhuravlev, A.Yu., Gámez Vintaned, J.A., and Liñán, E. 2011. The Palaeoscolecida and the evolution of the Ecdysozoa. *Palaeontographica Canadiana*, 31:177–204.

APPENDIX 1.

Absolute measures of *Hadimopanella oezgueli* dorsal-view sclerites from the Genestosa Member (PDF only).

APPENDIX 2.

Absolute measures of *Hadimopanella oezgueli* dorsal-view sclerites from other published papers (PDF only).

APPENDIX 3.

Dorsal relationships used in the establishment of morphotypes of *Hadimopanella oezgueli* from the Genestosa Member and other occurrences from published reports.

	Diameter relation			Diameter base surface	Diameter tuberculated surface	Eccentric deviation (ed)	Feature of tubercles			
Dorsal name	Dme / dme	Dme-d'me/D	d'-d/D	Dmax / Dmin	dmax / dmin	ed/dmax	nºtubercles/ dme	ø largest tubercle / ø tip	ø smallest tubercle / ø tip	ø largest tubercle/ ø smallest tubercle
HD-18-01	1.991	0.247	0.251	1.036	1.125	0.006	0.114	2.160	2.906	1.705
HD-3-01	1.390	0.146	0.135	1.050	1.235	0.090	0.129	4.460	3.215	1.631
HD-2-01	1.471	0.143	0.177	1.055	1.181	0.084	0.113	4.069	2.132	2.092
HD-34-01	1.839	0.196	0.261	1.042	1.294	0.103	0.000	3.712	2.208	2.157
HD-33-01	1.681	0.187	0.218	1.022	1.120	0.097	0.129	2.187	2.550	2.047
HD-5-01	2.088	0.276	0.245	1.111	1.182	0.238	0.098	6.153	4.300	1.951
HD-7-01	1.748	0.195	0.233	1.094	1.131	0.122	0.135	7.036	4.047	1.156
HD-21-01	1.460	0.096	0.219	1.046	1.082	0.082	0.311	–	–	1.602
HD-22-01	1.621	0.194	0.189	1.147	1.015	0.094	0.181	–	–	1.270
H1-01	1.558	0.155	0.203	1.109	1.057	0.083	0.117	–	–	2.800
H26-01	1.589	0.154	0.216	1.026	1.142	0.090	0.108	–	–	2.581
HD-9-01	1.644	0.164	0.228	1.086	1.196	0.069	0.124	–	–	1.581
HD-29-01	1.612	0.088	0.291	1.079	1.183	0.065	–	–	–	1.376
HD-12-01	1.524	0.100	0.244	1.028	1.236	0.052	0.175	–	–	1.967
H25-01	1.690	0.108	0.300	1.187	1.133	0.220	–	–	–	1.455
HD-10-01	1.607	0.167	0.211	1.091	1.210	0.089	–	–	–	–
HD-28-01	2.177	0.169	0.372	1.181	1.081	0.143	0.178	–	–	1.486
HD-24-01	1.780	0.123	0.315	1.089	1.100	0.128	0.136	–	–	1.766
HD-32-01	1.672	0.151	0.251	1.254	1.029	0.127	–	–	–	1.005
HD-39-01	1.672	0.113	0.163	1.254	1.029	0.126	–	–	–	1.070
HD-36-01	1.781	0.203	0.235	1.091	1.143	0.044	–	–	–	2.180
HD-1-01	1.681	0.082	0.323	1.109	1.038	0.048	–	–	–	–
HD-35-01	1.888	0.279	0.192	1.042	1.059	0.041	0.084	2.698	4.380	1.512
HD-14-01	1.369	0.065	0.205	1.187	1.267	0.032	0.084	4.002	2.415	1.141
HD-17-01	2.241	0.299	0.255	1.038	1.039	0.052	0.096	4.639	2.549	2.854
HD-15-01	1.576	0.121	0.245	1.047	1.158	0.055	0.107	6.631	3.336	2.369
H27-01	1.611	0.216	0.164	1.016	1.381	0.052	–	3.258	1.611	4.403
HD-4-01	2.404	0.314	0.270	1.074	1.172	0.049	0.128	2.264	1.756	1.658
HD-19-01	2.019	0.267	0.238	1.119	1.131	0.057	0.107	2.799	4.080	1.305
H10-01	1.880	0.283	0.185	1.034	1.023	0.062	0.146	2.614	2.177	1.471
H19-01	2.302	0.334	0.231	1.091	1.145	0.062	0.120	3.130	2.408	1.756
HD-41-01	1.999	0.242	0.258	1.074	1.150	0.022	–	–	–	–
HD-40-01	2.080	0.203	0.317	1.121	1.103	0.017	0.320	–	–	1.222
Mila1	1.690	0.221	0.187	1.086	1.113	0.114	0.032	5.645	–	–
Mila2	1.577	0.129	0.236	1.024	1.185	0.056	0.110	2.665	4.732	1.348
Mila3	1.960	0.256	0.234	1.063	1.083	0.026	0.057	4.167	3.231	1.216
Mila4	2.153	0.221	0.314	1.115	1.134	0.288	0.071	3.573	2.609	1.128

Mila5	1.959	0.247	0.243	1.123	1.090	0.140	0.106	3.583	–	–
Mila6	1.651	0.326	0.069	1.051	1.105	0.165	0.106	2.677	3.705	1.226
Mila7	1.665	0.209	0.190	1.032	1.087	0.136	0.049	2.688	–	–
Mila8	1.820	0.289	0.162	1.027	1.096	0.174	0.065	5.354	–	–
Mila9	1.730	0.294	0.129	1.161	1.034	0.240	0.065	3.379	–	–
Mila10	1.812	0.280	0.168	1.320	1.197	0.237	0.054	3.873	–	–
Mila11	1.678	0.111	0.293	1.110	1.113	0.122	0.128	8.379	–	–
Mila12	1.602	0.251	0.125	1.044	1.104	0.160	0.099	3.896	–	–
Ülgase-Kallavere1	1.566	0.158	0.203	1.093	1.050	0.164	0.024	–	–	1.338
Ülgase-Kallavere2	1.652	0.153	0.242	1.086	1.074	0.041	0.054	2.247	–	–
Ülgase-Kallavere3	1.563	0.197	0.163	1.192	1.281	0.118	0.044	4.057	2.829	1.230
Ülgase-Kallavere4	1.524	0.186	0.157	1.059	1.047	0.075	0.049	4.907	–	–
Ülgase-Kallavere5	1.398	0.217	0.068	1.081	1.038	0.078	0.058	–	–	1.291
Láncara1	1.657	0.192	0.205	1.019	1.156	0.110	0.119	2.362	1.766	1.994
Láncara2	1.680	0.191	0.214	1.123	1.025	0.023	0.089	2.991	2.214	1.770
Láncara3	1.865	0.194	0.270	1.022	1.127	0.071	0.112	0.000	–	1.664
Láncara4	1.715	0.226	0.191	1.159	1.007	0.055	0.100	3.332	1.976	1.431
Láncara5	1.613	0.197	0.184	1.173	1.014	0.012	0.060	2.220	3.406	1.197
Láncara6	1.639	0.262	0.128	1.153	1.089	0.067	0.020	4.227	3.677	1.048
Láncara7	1.425	0.169	0.129	1.067	1.148	0.078	0.052	3.548	–	–
Láncara8	1.291	0.110	0.115	1.455	1.367	0.087	0.059	4.441	2.636	1.508
Láncara9	1.681	0.249	0.156	1.260	1.110	0.060	0.102	4.083	–	–
Sinsk S1	1.557	0.218	0.139	1.126	1.054	0.126	0.178	6.582	5.881	1.506
Sinsk S2	1.314	0.121	0.118	1.094	1.054	0.079	0.289	8.637	–	–
Sinsk S3	1.387	0.089	0.190	1.059	1.063	0.086	0.316	3.258	–	–
Sinsk S4	1.874	0.203	0.263	1.208	1.265	0.255	0.189	6.426	–	–
Sinsk S5	1.949	0.189	0.298	1.110	1.105	0.026	0.214	4.521	–	–
Korrelasyon unda1	1.681	0.224	0.181	1.069	1.104	0.044	0.043	1.550	–	–
Sinsk Ps1	1.804	0.312	-0.134	1.037	1.093	0.727	0.190	11.080	4.179	1.157
Sinsk Ps2	1.565	0.273	-0.088	1.039	1.263	0.095	0.257	6.338	7.454	1.804
Sinks Ps3	1.817	0.227	-0.223	1.009	1.073	2.192	0.146	2.898	–	–
Monastery Greek1	0.745	0.185	0.168	1.142	1.224	0.110	0.437	2.164	2.630	1.200
Monastery Greek2	0.563	0.956	0.000	1.098	1.096	0.019	0.163	2.463	–	–
Campo Pisano	1.068	0.318	0.179	1.071	1.070	0.272	0.208	3.171	2.090	1.654
Çal Tepe 1	0.637	0.158	0.028	1.139	1.058	0.012	–	2.166	–	–
Çal Tepe 2	0.886	0.158	0.243	1.103	1.095	0.014	0.180	2.308	–	–
Çal Tepe 3	0.896	0.242	0.167	1.116	1.065	0.076	0.115	2.851	–	–

APPENDIX 4.

Absolute measures of *Hadimopanella oezgueli* lateral-view sclerites from the Genestosa Member.

Lateral name	ht	h	h1	h2	h3	d	r	α1	α2	α3
H38-01	55.671	40.523	11.654	12.266	16.603	138.81	69.405	30.583	48.013	50.711
H29-01	73.037	61.696	16.302	13.993	31.401	139.681	69.8405	56.564	52.5	39.145
H13-01	51.809	42.183	9.01	17.998	15.175	129.416	64.708	36.858	36.417	44.36
H32-01	60.671	37.346	13.414	9.935	13.997	140.827	70.4135	47.757	36.031	–
H21-01	64.839	47.617	11.099	20.12	16.398	135.281	67.6405	38.515	35.538	40.343
H9-01	73.868	45.555	13.951	11.46	20.144	123.545	61.7725	45.335	40.432	34.695
H30-01	79.495	65.154	17.624	22.536	24.994	173.338	86.669	48.93	42.057	69.391
H26-01	78.061	69.614	22.138	14.271	33.205	153.826	76.913	46.494	55.717	70.925
H25-01	63.85	49.856	16.617	–	33.239	146.276	73.138	44.66	–	42.272
H6-01	66.935	57.088	19.515	16.602	20.971	173.887	86.9435	40.173	40.024	61.048
H19-01	72.589	52.088	16.398	14.357	21.333	149.498	74.749	48.013	39.601	60.893
H23-01	74.558	62.272	18.843	14.351	29.078	158.569	79.2845	43.615	44.298	54.083
H1-01	78.031	55.29	29.089	11.042	15.159	168.057	84.0285	33.174	31.589	51.099
H20-01	48.381	37.305	14.348	7.374	15.583	166.076	83.038	31.19	26.453	30.41
H12-01	59.917	43.498	20.521	11.898	11.079	135.442	67.721	48.197	34.088	53.797
H3-01	65.257	55.409	18.876	18.888	17.645	176.173	88.0865	37.81	39.168	61.948
H34-01	66.006	54.938	16.813	21.312	16.813	161.535	80.7675	43.027	40.772	66.46
H31-01	65.6525	58.436	24.717	11.609	22.11	142.863	71.4315	50.964	46.97	60.962
H8-01	76.307	61.14	23.393	16.374	21.373	164.154	82.077	48.166	50.606	61.126
H10-01	48.783	48.783	17.217	5.74	25.826	158.711	79.3555	40.692	31.834	33.532
H28-01	51.557	38.738	11.067	–	27.671	115.131	57.5655	45.533	25.37	56.872
H24-01	76.744	58.684	20.144	8.574	29.966	156.628	78.314	39.983	34.176	34.176
H18-01	50.885	34.471	12.72	4.922	16.829	121.056	60.528	42.663	42.879	76.061
HP-3-01	60.786	50.08	18.916	12.896	18.268	150.822	75.411	49.7	48.747	41.174
HP-4-01	76.969	54.951	21.444	–	33.507	174.356	87.178	32.295	–	51.289
HP-5-01	53.484	39.921	10.492	9.085	20.344	132.091	66.0455	38.074	–	65.486
HP-6-01	53.961	42.709	10.486	5.964	26.259	114.546	57.273	47.85	–	69.391
HP-7-01	69.182	52.483	15.339	16.526	20.618	151.992	75.996	39.245	53.051	62.488
HP-9-01	48.564	34.506	9.713	8.928	15.865	117.862	58.931	35.191	32.475	63.258
HP-10-01	51.82	40.049	11.26	9.59	19.199	136.146	68.073	32.262	62.79	74.363
HP-11-01	52.927	41.419	9.974	10.096	21.349	113.808	56.904	46.231	47.778	68.091
HP-12-01	61.112	43.366	17.431	6.8	19.135	151.663	75.8315	28.955	40.488	56.066
HP-13-01	76.903	57.684	17.772	12.534	27.378	180.253	90.1265	36.457	38.412	50.236
HP-14-01	66.193	52.13	17.699	13.458	20.973	154.712	77.356	44.412	35.578	43.832
HP-15-01	47.047	35.028	8.185	13.032	13.811	116.204	58.102	50.528	44.297	67.655
HP-16-01	74.815	57.051	13.669	13.28	30.102	152.205	76.1025	42.346	47.041	62.045

APPENDIX 5.

Lateral relationships of *Hadimopanella oezgueli* from the Genestosa Member used for statistical analyses.

	Height relationship			Radius relationship	Slope relationship			Features tubercles
Nombre pefil	**h/h1**	**h/h2**	**h/h3**	**r/h**	**tg α1**	**tg α2**	**tg α3**	**base/tip**
H38-01	3.477	3.304	2.441	1.713	0.591	1.111	1.222	0.324
H29-01	3.785	4.409	1.965	1.132	1.515	1.303	0.814	0.242
H13-01	4.682	2.344	2.780	1.534	0.750	0.738	0.978	0.407
H32-01	2.784	3.759	2.668	1.885	1.101	0.727	–	0.308
H21-01	4.290	2.367	2.904	1.421	0.796	0.714	0.849	0.600
H9-01	3.265	3.975	2.261	1.356	1.012	0.852	0.692	0.318
H30-01	3.697	2.891	2.607	1.330	1.148	0.902	2.659	0.318
H26-01	3.145	4.878	2.096	1.105	1.054	1.467	2.892	0.121
H25-01	3.000	0.000	1.500	1.467	0.988	0.000	0.909	0.180
H6-01	2.925	3.439	2.722	1.523	0.844	0.840	1.808	0.412
H19-01	3.176	3.628	2.442	1.435	1.111	0.827	1.796	0.195
H23-01	3.305	4.339	2.142	1.273	0.953	0.976	1.381	0.201
H1-01	1.901	5.007	3.647	1.520	0.654	0.615	1.239	0.311
H20-01	2.600	5.059	2.394	2.226	0.605	0.498	0.587	0.277
H12-01	2.120	3.656	3.926	1.557	1.118	0.677	1.366	0.425
H3-01	2.935	2.934	3.140	1.590	0.776	0.815	1.877	0.379
H34-01	3.268	2.578	3.268	1.470	0.933	0.862	2.295	0.537
H31-01	2.364	5.034	2.643	1.222	1.233	1.071	1.801	0.279
H8-01	2.614	3.734	2.861	1.342	1.117	1.218	1.813	0.215
H10-01	2.833	8.499	1.889	1.627	0.860	0.621	0.663	0.192
H28-01	3.500	0.000	1.400	1.486	1.019	0.474	1.532	0.178
H24-01	2.913	6.844	1.958	1.335	0.839	0.679	0.679	0.311
H18-01	2.710	7.003	2.048	1.756	0.922	0.929	4.029	0.309
HP-3-01	2.647	3.883	2.741	1.506	1.179	1.140	0.875	0.395
HP-4-01	2.563	0.000	1.640	1.586	0.632	0.000	1.248	0.091
HP-5-01	3.805	4.394	1.962	1.654	0.783	0.000	2.193	0.227
HP-6-01	4.073	7.161	1.626	1.341	1.105	0.000	2.659	0.154
HP-7-01	3.422	3.176	2.545	1.448	0.817	1.330	1.920	0.172
HP-9-01	3.553	3.865	2.175	1.708	0.705	0.636	1.985	0.172
HP-10-01	3.557	4.176	2.086	1.700	0.631	1.945	3.573	0.214
HP-11-01	4.153	4.103	1.940	1.374	1.044	1.102	2.486	0.212
HP-12-01	2.488	6.377	2.266	1.749	0.553	0.854	1.486	0.336
HP-13-01	3.246	4.602	2.107	1.562	0.739	0.793	1.202	0.385
HP-14-01	2.945	3.874	2.486	1.484	0.980	0.715	0.960	0.201
HP-15-01	4.280	2.688	2.536	1.659	1.214	0.976	2.433	0.257
HP-16-01	4.174	4.296	1.895	1.334	0.911	1.074	1.884	0.141

APPENDIX 6.

Histogram values: (1) maximum diameters measured in dorsal view sclerites; (2) heights measured in lateral view sclerites.

Dorsal name	Major diameter (Dmax) µm	Lateral name	height µm
HD-18-01	142.337	H38-01	40.523
HD-3-01	154.42	H29-01	61.696
HD-2-01	120.553	H13-01	42.183
HD-34-01	153.179	H32-01	37.346
HD-33-01	145.331	H21-01	47.617
HD-5-01	157.005	H9-01	45.555
HD-7-01	162.709	H30-01	65.154
HD-21-01	134.524	H26-01	69.614
HD-22-01	124.077	H25-01	49.856
H1-01	153.76	H6-01	57.088
H26-01	133.944	H19-01	52.088
HD-9-01	137.934	H23-01	62.272
HD-29-01	138.783	H1-01	55.29
HD-12-01	167.938	H20-01	37.305
H25-01	137.6	H12-01	43.498
HD-10-01	152.557	H3-01	55.409
HD-28-01	159.201	H34-01	54.938
HD-24-01	136.114	H31-01	58.436
HD-32-01	154.497	H8-01	61.14
HD-39-01	164.546	H10-01	48.783
HD-36-01	133.911	H28-01	38.738
HD-1-01	145.65	H24-01	58.684
HD-35-01	182.392	H18-01	34.471
HD-14-01	123.954	HP-3-01	50.08
HD-17-01	190.261	HP-4-01	54.951
HD-15-01	180.714	HP-5-01	39.921
H27-01	146.566	HP-6-01	42.709
HD-4-01	194.65	HP-7-01	52.483
HD-19-01	179.787	HP-9-01	34.506
H10-01	144.161	HP-10-01	40.049
H19-01	199.513	HP-11-01	41.419
HD-41-01	172.599	HP-12-01	43.366
HD-40-01	178.53	HP-13-01	57.684
		HP-14-01	52.13
		HP-15-01	35.028
		HP-16-01	57.051